Scaling analysis in Fourier and Walsh-Rademacher basis systems

A. A. Kutsenko, K. Bellinghausen, S. Danilov, S. Juricke, and M. Oliver

CU Bremen, KU Ingolstadt, AWI Bremerhaven, Germany

March 28, 2023

Different "scaled" bases in one space

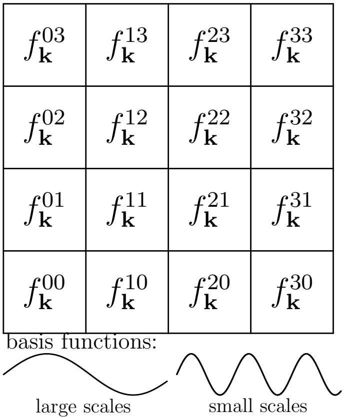

Fourier system $\mathbf{f_k}$

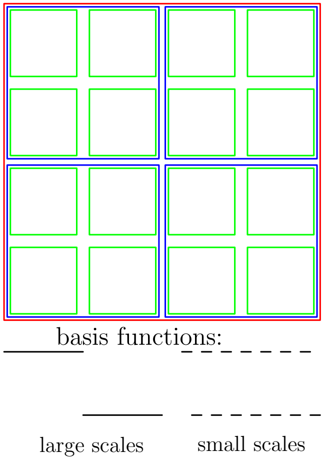

Walsh-Rademacher system $\mathbf{g_k}$

Figure: The same field can be expanded in two basis systems $u = \sum u_{\mathbf{k}} \mathbf{f_k} = \sum v_{\mathbf{k}} \mathbf{g_k}$, where $\mathbf{k}$ is a scaling parameter.

Different "ordered" bases in one space - WR basis

1) Walsh-Rademacher basis. Spaces of piece-wise constant functions on $[0,1)^d$:

$$\mathcal{W}_{[0,1)} \subset \mathcal{W}_{[0,2)} \subset \mathcal{W}_{[0,4)} \subset \mathcal{W}_{[0,8)} \subset \ldots \subset \mathcal{W}_{[0,2^N)} \quad :$$

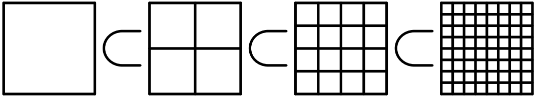
and so on

Thus, denoting $\mathcal{W}_{[2^n,2^{n+1})} = \mathcal{W}_{[0,2^{n+1})} \ominus \mathcal{W}_{[0,2^n)}$, we can write

$$\mathcal{W}_{[0,2^N)} = \mathcal{W}_{[0,1)} \oplus \mathcal{W}_{[1,2)} \oplus \mathcal{W}_{[2,4)} \oplus \mathcal{W}_{[4,8)} \oplus \ldots \oplus \mathcal{W}_{[2^{N-1},2^N)}.$$

Then, we take the "ordered" orthonormal Walsh-Rademacher basis $\mathrm{bas}\mathcal{W}_{[0,2^N)} = \{g_{\mathbf{k}}\}_{0 \leqslant |\mathbf{k}| < 2^N}$, where

$$\mathrm{bas}\mathcal{W}_{[2^{n-1},2^n)} = \{g_{\mathbf{k}}\}_{2^{n-1} \leqslant |\mathbf{k}| < 2^n}.$$

Remark. While $\mathcal{W}_{[2^{n-1},2^n)}$ is defined uniquely, $\{g_{\mathbf{k}}\}_{2^{n-1} \leqslant |\mathbf{k}| < 2^n}$ is not unique, but the range $2^{n-1} \leqslant |\mathbf{k}| < 2^n$ is unique.

Different "ordered" bases in one space - F basis

$f_{\mathbf{k}}^{03}$	$f_{\mathbf{k}}^{13}$	$f_{\mathbf{k}}^{23}$	$f_{\mathbf{k}}^{33}$
$f_{\mathbf{k}}^{02}$	$f_{\mathbf{k}}^{12}$	$f_{\mathbf{k}}^{22}$	$f_{\mathbf{k}}^{32}$
$f_{\mathbf{k}}^{01}$	$f_{\mathbf{k}}^{11}$	$f_{\mathbf{k}}^{21}$	$f_{\mathbf{k}}^{31}$
$f_{\mathbf{k}}^{00}$	$f_{\mathbf{k}}^{10}$	$f_{\mathbf{k}}^{20}$	$f_{\mathbf{k}}^{30}$

Figure: 2) Fourier basis in $\mathcal{W}_{[0,2^N)}$ is the standard discrete Fourier basis $e^{i\mathbf{k}\cdot\mathbf{x}}$ taken at the lattice points $\{(f_{\mathbf{k}}^{ij})\}_{\mathbf{k}\in\mathbb{Z}_{2N}^d}$ extended to the squares constantly. Again, $0 \leqslant |\mathbf{k}| < 2^N$.

Different bases give different slopes for random fields

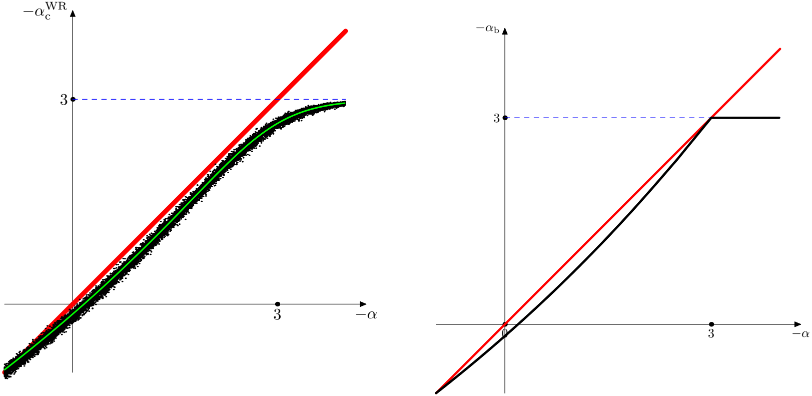

number of small squares

$N = 100 \times 100$

resolution $N \to \infty$

Figure: Random fields with $\sum_{|\mathbf{k}|=K} |u_{\mathbf{k}}|^2 \simeq K^\alpha$ in F-basis have different slope in WR-basis, namely

$$\alpha_{\mathrm{b}} \to -1 + \log_2 \frac{\int\limits_{[0,\pi/2]^d} |\mathbf{x}|^{1-d+\alpha}(1-\prod_{j=1}^d \cos^2 x_j)\,d\mathbf{x}}{\int\limits_{[0,\pi/2]^d} |\mathbf{x}|^{1-d+\alpha}(1-\prod_{j=1}^d \cos^2 2x_j)\prod_{j=1}^d \cos^2 x_j\,d\mathbf{x}}, \text{ for } N \to \infty.$$

F- and WR-slopes are different but the cumulative energy is similar. Example - continuous case

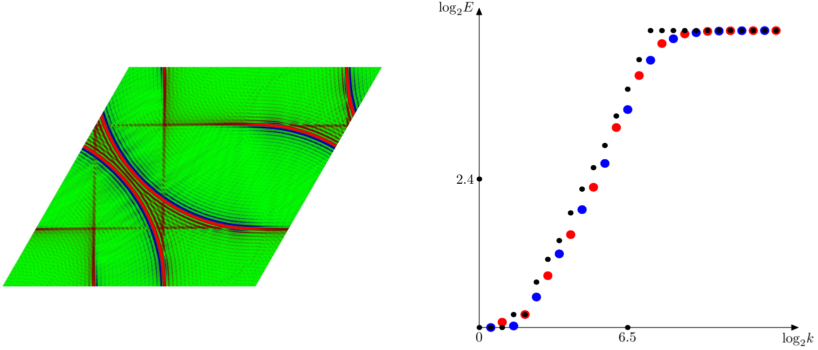

cumulative energy

Figure: More complex field. Black dots - continuous F, red - rhombus WR, blue - triangular WR. Logarithm of L^2-norm of the projection on the scales $[0, k)$ is plotted.

F- and WR-slopes are different but the cumulative energy is similar. Example - continuous case

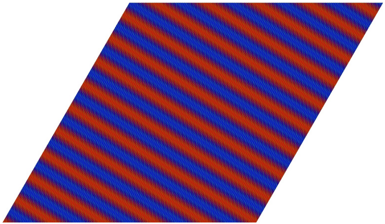

$$u(x, y) = \cos\left(2\pi \cdot 5x + \frac{4\pi \cdot 7y}{\sqrt{3}}\right) + \cos\left(2\pi \cdot 131x + \frac{4\pi \cdot 503y}{\sqrt{3}}\right)$$

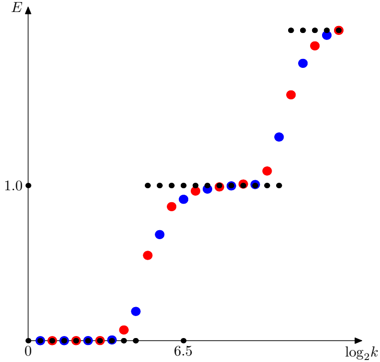

cumulative energy

Figure: Two simple harmonics. Black dots - continuous F, red - rhombus WR, blue - triangular WR. L^2-norm of the projection on the scales $[0, k)$ is plotted.

F- and WR-slopes are different but the cumulative energy is similar. Example - continuous case

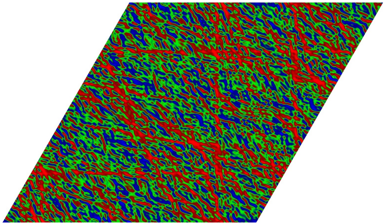

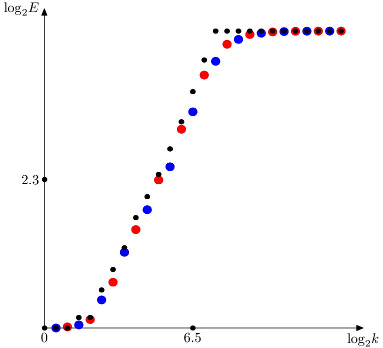

cumulative energy

Figure: More complex field. Black dots - continuous F, red - rhombus WR, blue - triangular WR. Logarithm of L^2-norm of the projection on the scales $[0, k)$ is plotted.

Reverse case: F-diagnostics of random WR-fields

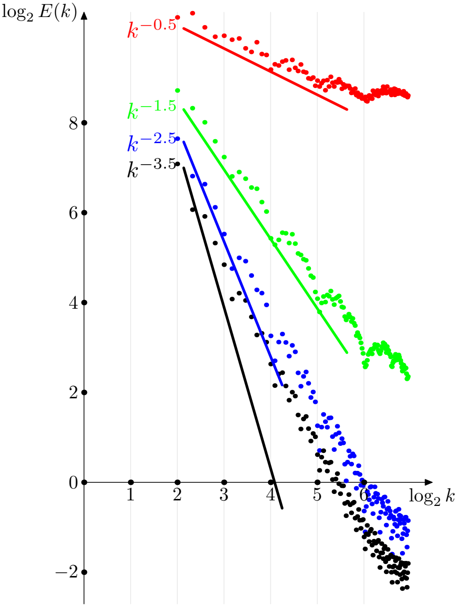

Original slopes in WR-basis are presented by solid lines, their F-diagnostics are dots. 2000 random WR-fields at resolution 256×256 are generated for each of the slopes, then the average of all the F-diagnostics is taken.

Fourier basis already "fails" for the slopes around k^{-2}!

Practical applications

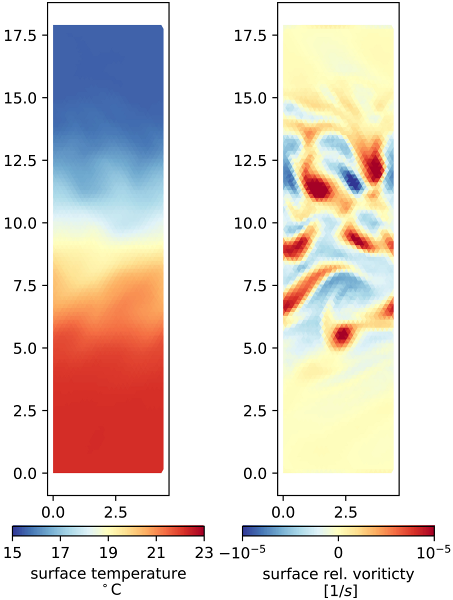

Figure: Simulations of a zonal flow in a channel. *Juricke et al. 2022*

Practical applications

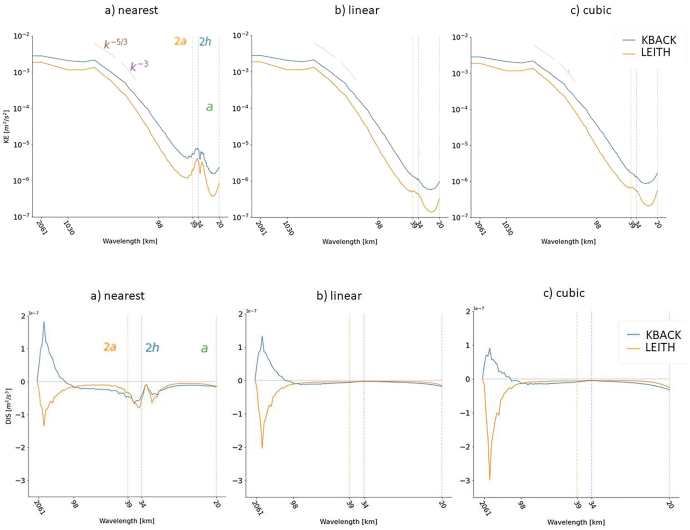

Figure: F-diagnostics of energy and dissipation power spectra. Different methods of interpolations give slightly different results.

Practical applications

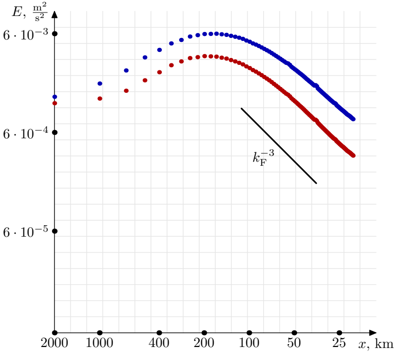

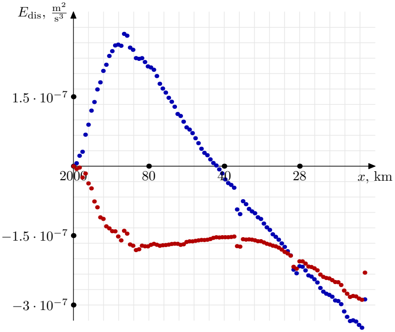

Figure: Energy and dissipation power spectra computed by the modified resize-and-average method. Blue points correspond to backscatter parametrization, red points to the Leith parametrization.

Conclusion and perspectives

The computation of WR-spectra is almost simple and based on the ideas: select regions, resize [optional, to resolve k between powers of 2], and average. Intel IPP provides highly optimized routines for the image processing which can be adapted for WR-diagnostics.

A generalization of the results to unstructured meshes, to incomplete (sparse) data - almost done.

More interesting mathematical ideas and beautiful formulas.